JACS Au
AN OPEN ACCESS JOURNAL OF THE AMERICAN CHEMICAL SOCIETY

pubs.acs.org/jacsau

Article

Azide-Masked Fluorescence Turn-On Probe for Imaging Mycobacteria

Sajani H. Liyanage, N. G. Hasitha Raviranga, Julia G. Ryan, Scarlet S. Shell, Olof Ramström, Rainer Kalscheuer, and Mingdi Yan*

Cite This: *JACS Au* 2023, 3, 1017−1028

Read Online

ACCESS | Metrics & More | Article Recommendations | Supporting Information

ABSTRACT: A fluorescence turn-on probe, an azide-masked and trehalose-derivatized carbazole (**Tre-Cz**), was developed to image mycobacteria. The fluorescence turn-on is achieved by photoactivation of the azide, which generates a fluorescent product through an efficient intramolecular C−H insertion reaction. The probe is highly specific for mycobacteria and could image mycobacteria in the presence of other Gram-positive and Gram-negative bacteria. Both the photoactivation and detection can be accomplished using a handheld UV lamp, giving a limit of detection of 10^3 CFU/mL, which can be visualized by the naked eye. The probe was also able to image mycobacteria spiked in sputum samples, although the detection sensitivity was lower. Studies using heat-killed, stationary-phase, and isoniazid-treated mycobacteria showed that metabolically active bacteria are required for the uptake of **Tre-Cz**. The uptake decreased in the presence of trehalose in a concentration-dependent manner, indicating that **Tre-Cz** hijacked the trehalose uptake pathway. Mechanistic studies demonstrated that the trehalose transporter LpqY-SugABC was the primary pathway for the uptake of **Tre-Cz**. The uptake decreased in the LpqY-SugABC deletion mutants Δ*lpqY*, Δ*sugA*, Δ*sugB*, and Δ*sugC* and fully recovered in the complemented strain of Δ*sugC*. For the mycolyl transferase antigen 85 complex (Ag85), however, only a slight reduction of uptake was observed in the Ag85 deletion mutant Δ*Ag85C*, and no incorporation of **Tre-Cz** into the outer membrane was observed. The unique intracellular incorporation mechanism of **Tre-Cz** through the LpqY-SugABC transporter, which differs from other trehalose-based fluorescence probes, unlocks potential opportunities to bring molecular cargoes to mycobacteria for both fundamental studies and theranostic applications.

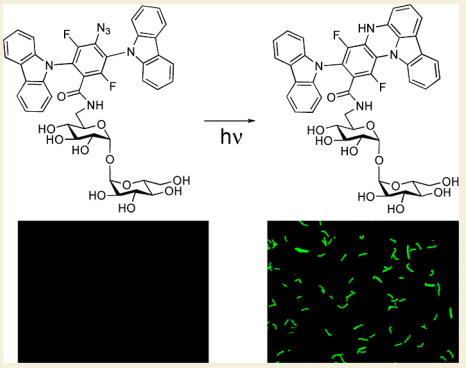

KEYWORDS: *Mycobacteria, trehalose, fluorescence turn-on, aryl azide, LpqY-SugABC*

1. INTRODUCTION

Tuberculosis (TB), caused by the bacterial pathogen *Mycobacterium tuberculosis*, is a top infectious disease. According to the World Health Organization Global Tuberculosis Report, approximately 10.6 million people developed TB and more than 1.6 million died in 2021 due to the reduced access to TB diagnosis and treatment.[1] It is well known that early diagnosis is critical for disease prognosis and reducing death.[2−4] Among the methods to detect mycobacteria in vitro and in vivo, the most accurate is culturing the bacteria in growth medium. However, this method is time-consuming as it can take weeks to grow *M. tuberculosis*.[5−8] More than a century ago, microscopic observation of bacilli that uses Ziehl−Neelsen staining was invented.[9,10] The method, so-called acid-fast staining, involves applying a primary dye (carbol fuchsin), a decolorizer (acid alcohol), and a counterstain (methylene blue) to the smear sample on a glass slide and viewing under a microscope.[11] For resource-limited countries, this has become a cost-effective way to detect *M. tuberculosis* in sputum. The drawbacks of this method include the time-consuming procedure, relatively low sensitivity (50−60%), and even lower sensitivity in HIV co-infected patient samples.[12,13] Nucleic acid-based diagnostic tools such as GeneXpert provide high sensitivity and reliability when combined with a DNA amplification system.[14] The high cost and the requirement of skilled technical personnel make it difficult to adopt this tool in resource-limited settings. Also, this method cannot assess the viability of bacteria, an important factor that may affect treatment decisions.[12,15]

Fluorescent probes have become a prevalent tool for cell imaging. Organic fluorophores are among the most popular fluorescent probes due to the availability of a wide selection of structures having different excitation and emission characteristics. A major drawback of organic fluorophores is photobleaching, where the fluorophore loses its ability to fluoresce,

Received: August 12, 2022
Revised: February 17, 2023
Accepted: February 17, 2023
Published: March 27, 2023

https://doi.org/10.1021/jacsau.2c00449
JACS Au 2023, 3, 1017−1028

Scheme 1. Transport and Utilization of Trehalose in Mycobacteria[a]

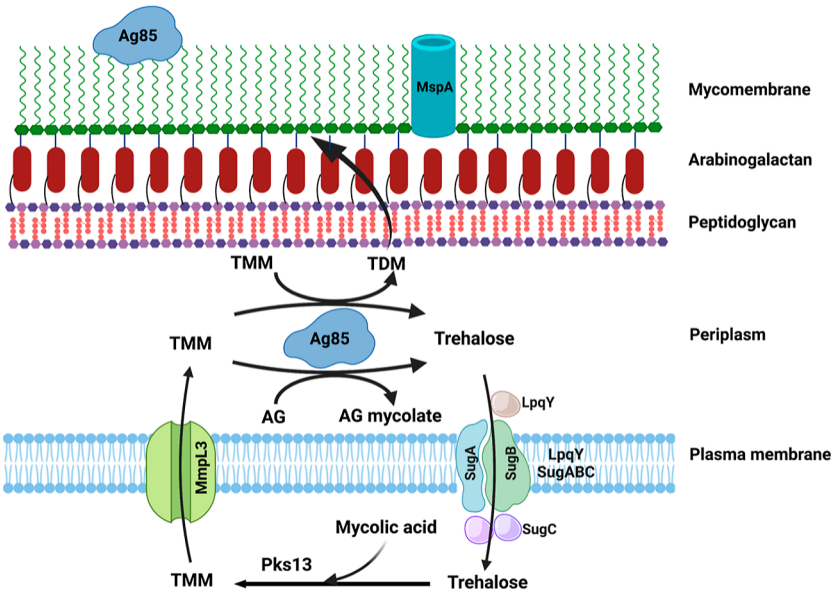

[a]The scheme was created with BioRender.com

especially under continuous light irradiation. Photobleaching causes permanent alteration to the fluorophore structure, and hence, the fluorescence cannot be recovered once the molecule is photobleached. One strategy to minimize photobleaching is fluorescence turn-on, where the precursor molecule either shows low fluorescence or is non-fluorescent, and the fluorescence increases drastically when an external stimulus is applied. As the fluorescence is turned on only at the time of analysis, it drastically reduces the unnecessary light exposure of the fluorophore, thus minimizing photobleaching. The fluorophore can be masked, for example, by using solvatochromic dyes[16] or photosensitive functional groups[17] or through self-assembly of molecules,[18] fluorescence resonance energy transfer (FRET),[19,20] or enzymatic reactions.[15,21−26]

Fluorescence turn-on probes have been developed to detect mycobacteria.[15] Cirillo and co-workers designed a fluorescence turn-on probe by conjugating the fluorescent dye Cy5 with a fluorescence quencher linked through a β-lactam ring.[19] The probe was not fluorescent, but the fluorescence was turned on after the β-lactam was hydrolyzed by β-lactamase in mycobacteria. In another example, Rao and co-workers designed a series of fluorogenic substrate probes of cephalosporin lactams that are specific for BlaC, an enzyme that belongs to the class A lactamase family expressed by mycobacteria.[15,27] When the probe is hydrolyzed by BlaC, it releases hydrolyzed β-lactam and the fluorescent umbelliferone.

Fluorescence turn-on probes based on the action of trehalose have been developed to image mycobacteria.[28,29] Trehalose, a disaccharide consisting of two D-glucose units linked by an α-1,1-glycosidic bond, is essential for the survival and pathogenicity of *M. tuberculosis*.[30] On the other hand, trehalose is completely absent in the mammalian biology, and for these reasons, hijacking the trehalose transport and utilization pathways has become an attractive strategy in the development of therapeutics and imaging tools.[31] Scheme 1 shows the major pathways for the transport and utilization of trehalose in mycobacteria.[31] Exogenous trehalose is transported into the periplasm by the transmembrane porin in the mycomembrane, i.e., the outer membrane of the mycobacterium. In *Mycobacterium smegmatis*, the general porin MspA has an inner diameter of 4.9 nm and is 9.6 nm long.[32,33] Trehalose is also produced during the cell wall synthesis when the mycolyl transferase, antigen 85 complex (Ag85), transfers the mycolyl group in trehalose monomycolate (TMM) to arabinogalactan (AG) or another TMM to produce AG mycolate and trehalose dimycolate (TDM).[34,35] The periplasmic trehalose is then translocated into the cytoplasm by the ATP-binding cassette transporter LpqY-SugABC, where trehalose is either metabolized or converted to TMM.[36] LpqY has a distinct substrate preference for trehalose, and LpqY-SugABC does not utilize monosaccharides or other disaccharides such as maltose, a disaccharide of two D-glucose units linked by a β-1,1-glycosidic bond.[36,37] The mycolyl transferase Ag85 has been shown to tolerate structure modifications, such as trehalose derivatized with groups from small (azide) to large (fluorescein).[38,39] LpqY-SugABC, however, is less tolerant. Very few trehalose derivatives, all bearing modification by small groups like azido or deoxyfluoro, can be transported through the LpqY-SugABC pathway.[40−43]

Several fluorescence turn-on probes based on the action of trehalose have been reported, including solvatochromic dyes,[44−46] quencher-fluorophore,[47] molecular rotor turn-on fluorophore,[48] FRET,[49] or through enzyme action.[50] The solvatochromic dye-derivatized trehalose probe developed by Bertozzi and co-workers was incorporated into the mycomembrane through the action of Ag85.[44] The solvatochromic dye was non-fluorescent in the polar environment but became fluorescent in the lipophilic mycomembrane. The authors also found that the trehalose probe did not inhibit bacterial growth or perturb the functions of mycobacteria. The probe developed by Kiessling and co-workers has a quencher−trehalose−fluorophore construct and is also a substrate of Ag85.[47] Hydrolysis of the probe by Ag85 released the fluorophore, thus the fluorescence turn-on.

In this work, we report a fluorescence turn-on probe, a trehalose-derivatized carbazole (**Tre-Cz**), for the imaging of mycobacteria. The azido carbazole itself is minimally

https://doi.org/10.1021/jacsau.2c00449
JACS Au 2023, 3, 1017−1028

Scheme 2. Synthesis of Tre-Cz and Mal-Cz and the Photochemical Conversion of Tre-Cz to the Fluorescent Product P[a]

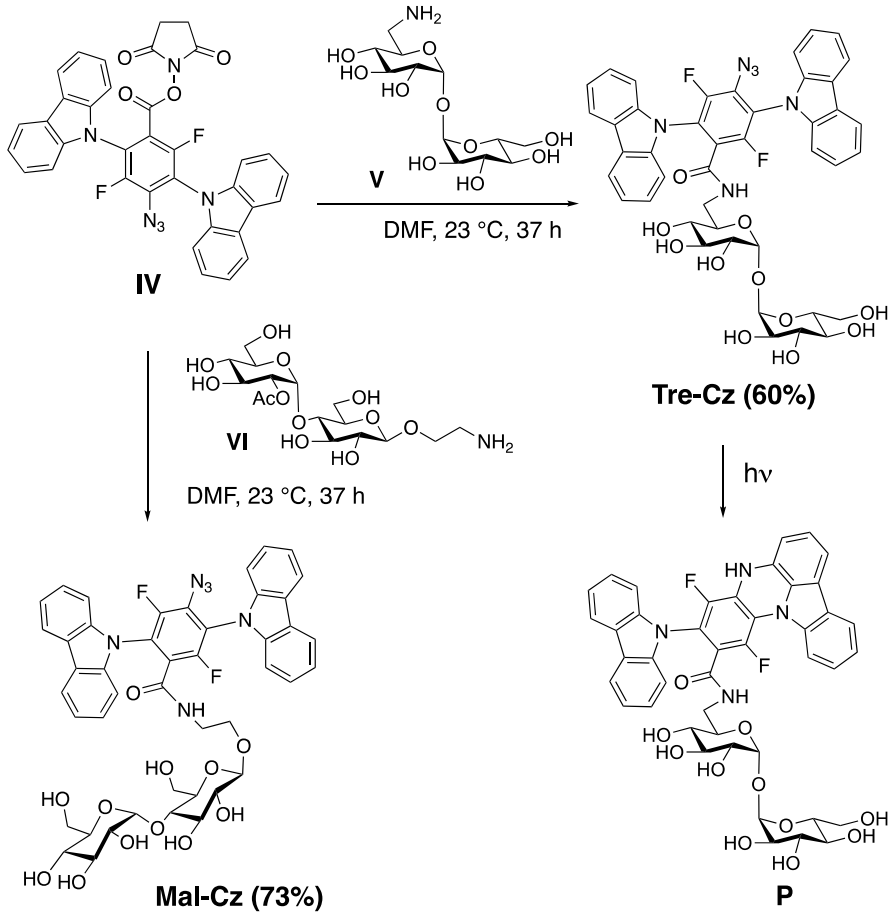

[a]See the Supporting Information for the syntheses of **IV**, **V**, and **VI**. DMF: *N*,*N*-dimethylformamide.

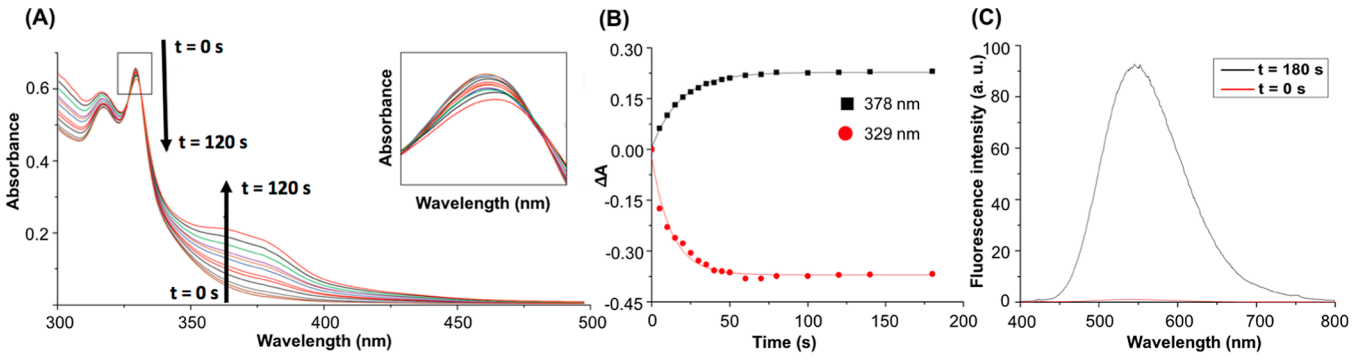

Figure 1. (A) Absorption spectra of **Tre-Cz** before and after irradiating a solution of **Tre-Cz** in methanol (50 μM) with a handheld UV lamp (intensity: 0.5 mW/cm^2 at 365 nm) every 10 s for a total of 120 s. Direction of arrows indicates increasing irradiation time. Inset is the expanded region showing decreases of absorbance at 329 nm with increasing irradiation time. (B) Change of absorbance at 329 and 378 nm vs irradiation time. The red and black curves are the first-order exponential decay fits of the experimental data. (C) Fluorescence spectra of **Tre-Cz** in methanol (50 μM) before (red) and after irradiation with a handheld UV lamp for 180 s (black). Excitation: 378 nm.

fluorescent. Photoactivation of the aryl azide generates the singlet nitrene, which reacts with the neighboring aryl ring through a C−H insertion reaction to form a fluorescent product **P** (Scheme 2).[17,51,52] We show that **Tre-Cz** was taken up by metabolically active mycobacteria, and the uptake was dependent on LpqY-SugABC. **Tre-Cz** is highly specific to mycobacteria and was able to image mycobacteria in the presence of other Gram-positive and Gram-negative bacteria, as well as mycobacteria in sputum.

2. RESULTS AND DISCUSSION

2.1. Synthesis of Tre-Cz and Mal-Cz

Mal-Cz, the maltose (Mal) analogue of **Tre-Cz**, was used as a negative control. Mal is a disaccharide consisting of two glucose units just like trehalose but has an α-1,4-glycosidic linkage instead of an α-1,1-glycosidic linkage in trehalose. Unlike trehalose, maltose is not a substrate for Ag85 and is not utilized by LpqY-SugABC.[36,37]

https://doi.org/10.1021/jacsau.2c00449
JACS Au 2023, 3, 1017−1028

Tre-Cz was prepared by coupling the amine-derivatized trehalose **V** (Scheme S1)[53−55] with the *N*-hydroxysuccinimide (NHS)-functionalized carbazole **IV** (Scheme S3).[17,56] The reaction was carried out at room temperature, giving **Tre-Cz** in 60% yield (Scheme 2). The corresponding **Mal-Cz** was synthesized in the same manner as **Tre-Cz** by coupling **IV** with an amine-derivatized Mal (**VI**, Scheme S2)[57−59] in 73% yield (Scheme 2). The structure of **Tre-Cz** was confirmed by ^{1}H NMR (Figures S50 and S51), IR (Figure S52), ^{19}F NMR (Figure S53), ^{13}C NMR (Figure S54), 2D COSY NMR (Figure S55), and high-resolution mass spectrometry (Figure S56). The ^{1}H NMR spectrum of **Tre-Cz** contains the characteristic anomeric protons in trehalose at 4.72 and 4.76 ppm and the aromatic protons of the carbazole at 7.00−8.10 ppm. The IR spectrum contains the characteristic azide peak at 2121 cm^{-1}.

2.2. Photophysical Properties of Tre-Cz

The photoconversion reaction of **Tre-Cz** was carried out by irradiating a solution of **Tre-Cz** in methanol using a medium-pressure Hg lamp (Scheme 2). The azide peak in **Tre-Cz** at 2121 cm^{-1} disappeared after conversion to the fluorescent photoproduct **P** (Figure S57). The ^{1}H NMR spectrum of **P** (Figure S58) showed the appearance of the amine proton at 9.06 ppm resulting from the insertion reaction of the aryl nitrene into the neighboring C−H bond.

The absorption maximum of **Tre-Cz** at 329 nm red-shifted to 378 nm after photoconversion to **P** (Figure S1). The kinetics of the photochemical reaction was monitored by UV−vis spectroscopy by irradiating a solution of **Tre-Cz** with a handheld UV lamp at 365 nm every 10 s for a total of 120 s. With increasing irradiation time, the λ_{max} value of **Tre-Cz** at 329 nm decreased, while the λ_{max} value of the photoproduct **P** at 378 nm increased (Figure 1A,B).

Tre-Cz was minimally fluorescent, whereas the photoproduct **P** was highly fluorescent with an emission maximum at 545 nm at 378 nm excitation (Figure 1C). The fluorescence intensity of the photoproduct was ∼90 times higher than that of **Tre-Cz** after 180 s of irradiation (Figure 1C).

The photophysical properties of **Tre-Cz** and **Mal-Cz** are summarized in Table 1. The photoconversion quantum yield (ϕ_P) was calculated from the kinetic curves of the reaction (Figures 1B and S2B) (see the Supporting Information for calculations). The results, 0.14 and 0.13, respectively, are comparable to those of the reported photoactivable azides.[60,61] The half-life of the photoconversion reaction was calculated to be 12 s (**Tre-Cz**) and 13 s (**Mal-Cz**) by fitting the kinetic curves to the first-order kinetic model (details in the Supporting Information).

Table 1. Absorption and Emission Parameters of Tre-Cz, Mal-Cz, and Their Photoproducts[a]

	λ_{abs} (nm) (ε_{max} ($M^{-1}cm^{-1}$))	λ_{abs}^{P} (nm)	λ_{em} (nm)	$t_{1/2}$ (s)	ϕ_P (λ_P)
Tre-Cz	329 (12,800)	378	545	12	0.14
Mal-Cz	330 (11,400)	372	541	13	0.13

[a]All measurements were done in methanol. λ_{abs}: absorption maximum of **Tre-Cz** or **Mal-Cz**. The molar absorption coefficient, ε, was calculated using the concentration series of each reactant. λ_{abs}^{P}: absorption maximum of photoproduct. λ_{em}: fluorescence emission of photoproduct. $t_{1/2}$: photoconversion half-life.

2.3. Uptake of Tre-Cz and Optimization of Conditions

M. smegmatis mc^{2}155 was selected for this study as it is a widely used model bacterium for *M. tuberculosis* and other mycobacterium species.[62] *M. smegmatis* mc^{2}155 has the same broad cell envelope architecture as *M. tuberculosis* and encodes thousands of conserved mycobacterial gene orthologs.[34,63−66] In both *M. tuberculosis* and *M. smegmatis*, TMM is synthesized in the cytoplasm from trehalose produced by three redundant trehalose biosynthesis pathways.[35,67] Free trehalose is also imported into the cytoplasm by LpqY-SugABC that is conserved in *M. tuberculosis* and *M. smegmatis*.[36] Given these similarities in cell envelope composition and usage of trehalose, we therefore considered *M. smegmatis* to be an appropriate model for the initial development and optimization of our probe.

A series of experiments were carried out to optimize the uptake conditions, including the incubation time (0.5−24 h), irradiation time (0.5−7 min), and probe concentration (50−600 μM). Briefly, *M. smegmatis* mc^{2}155 (10^{8} CFU/mL) was incubated with **Tre-Cz**. The cell pellet was collected by centrifugation, washed with pH 7.4 phosphate-buffered saline (PBS) twice to remove excess **Tre-Cz**, re-dispersed in PBS, and irradiated with a UV lamp at 365 nm. The fluorescence intensity of the cell pellet increased with the incubation time and plateaued after 6 h (Figure S3A). Even after 1 h of incubation, the fluorescence intensity was sufficiently strong, at >50% of the maximum. We then used the 1 h incubation time and monitored the fluorescence intensity vs the irradiation time. The fluorescence turn-on was rapid, reaching over 90% of the maximal intensity after only 30 s of irradiation (Figure S3B). Irradiation times longer than 1 min resulted in a decrease in fluorescence, likely due to photobleaching of the fluorescent product. The concentration study showed that ∼95% of the maximal fluorescence intensity was reached at 100 μM **Tre-Cz** and plateaued at 150 μM **Tre-Cz** and higher (Figure S3C). For the subsequent studies, the conditions of 1 h incubation time, 1 min irradiation, and 100 μM **Tre-Cz** concentration were used unless otherwise noted.

2.4. Uptake of Tre-Cz Is Specific for Mycobacteria

In addition to *M. smegmatis* mc^{2}155, *M. tuberculosis* H37Ra, an attenuated strain of *M. tuberculosis*,[68] was also tested. Similar to *M. smegmatis* mc^{2}155, the fluorescence increased with the concentration of **Tre-Cz** (Figure 2A). Unlike *M. smegmatis* mc^{2}155 where the fluorescence intensities plateaued at 150 μM (Figure S3C), the fluorescence intensities continued to increase in the case of *M. tuberculosis* H37Ra up to 500 μM. The reason for this slow uptake was that *M. tuberculosis* H37Ra is a considerably slow-growing strain, taking 16 days to reach an OD_{600} of 0.5 compared to 2 days for *M. smegmatis* mc^{2}155. This was also reflected in the lower fluorescence intensities of *M. tuberculosis* H37Ra than that of *M. smegmatis* mc^{2}155 at the same concentration of **Tre-Cz**.

Several experiments were conducted to confirm that the uptake of **Tre-Cz** is specific for mycobacteria. In the first experiment, other bacteria were tested, including the Gram-negative *Escherichia coli* and *Pseudomonas aeruginosa* and the Gram-positive *Staphylococcus epidermidis*. Compared to mycobacteria, these bacteria showed minimal fluorescence (Figure 2B). Second, **Tre-Cz** was added to mixed cultures of *M. smegmatis*, *E. coli*, *S. epidermidis*, and *P. aeruginosa* at different concentrations of *M. smegmatis* while keeping the concentration of the other three bacteria constant at 10^{8} CFU/

https://doi.org/10.1021/jacsau.2c00449
JACS Au 2023, 3, 1017−1028

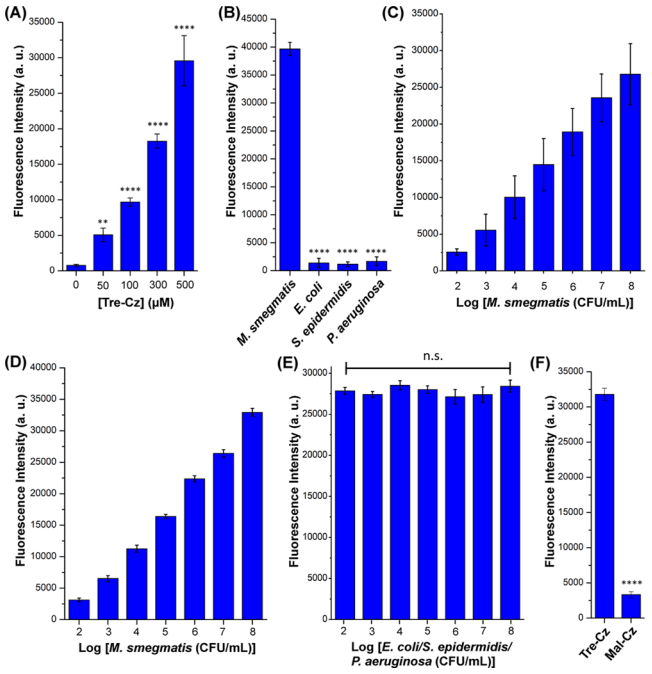

Figure 2. Uptake of **Tre-Cz** is specific for mycobacteria. (A) Fluorescence intensity of *M. tuberculosis* H37Ra (10^8 CFU/mL) after treating with different concentrations of **Tre-Cz** (0−500 μM). (B) Fluorescence intensity of *M. smegmatis* mc^{2}155, *S. epidermidis* ATCC 35984, *P. aeruginosa* PAO1, and *E. coli* ATCC 25922 after treating with **Tre-Cz**. The concentration of all bacteria strains was 10^8 CFU/mL. (C) Fluorescence intensity of mixed bacteria of *M. smegmatis*, *S. epidermidis*, *P. aeruginosa*, and *E. coli* after incubating with **Tre-Cz** at different concentrations of *M. smegmatis* (10^2−10^8 CFU/mL) and fixed concentrations of the other three strains (each at 10^8 CFU/mL). (D) Fluorescence intensity of different concentrations of *M. smegmatis* mc^{2}155 incubated with **Tre-Cz**. (E) Fluorescence intensity of mixed bacteria incubated with **Tre-Cz** at different concentrations of *E. coli*, *S. epidermidis*, and *P. aeruginosa* (each at 10^2−10^8 CFU/mL) and a fixed concentration of *M. smegmatis* (10^8 CFU/mL). (F) Uptake of **Tre-Cz** or **Mal-Cz** (100 μM) by *M. smegmatis* mc^{2}155 (10^8 CFU/mL). The fluorescence intensity of the bacteria only was subtracted from each data point. Results are presented as means ± standard error of the mean (SEM) of three independent experiments. Data were analyzed by one-way analysis of variance (ANOVA) (*P < 0.1, **P < 0.01, ***P < 0.001, ****P < 0.0001, n.s.: not significant, and P > 0.05). Groups were compared to (A) [**Tre-Cz**] = 0, (B) *M. smegmatis*, and (F) **Tre-Cz**.

mL. In this case, the fluorescence intensity increased with the concentration of *M. smegmatis* (Figure 2C). This is consistent with the result on *M. smegmatis* mc^{2}155 only that the fluorescence intensity increased with the concentration of *M. smegmatis* (Figure 2D), indicating that other bacteria did not interfere with the uptake of **Tre-Cz** by *M. smegmatis*. In the third experiment, the concentration of *M. smegmatis* was kept constant, while the concentrations of the other three bacteria varied. No change in the fluorescence intensity was observed in this case (Figure 2E). This result demonstrates that the uptake of **Tre-Cz** by *M. smegmatis* was not affected by the presence of other bacteria, again supporting the conclusion that the uptake of **Tre-Cz** is specific for mycobacteria.

The fourth experiment tested the substrate specificity by treating *M. smegmatis* mc^{2}155 with **Mal-Cz**. Compared to **Tre-Cz**, the fluorescence of **Mal-Cz**-treated *M. smegmatis* was minimal (Figure 2F). Even at high concentrations of **Mal-Cz** up to 5 mM, the fluorescence was still low, and unlike **Tre-Cz**, no concentration-dependent uptake was observed (Figure S4).

2.5. Fluorescence Turn-On Imaging of Mycobacteria

M. smegmatis mc^{2}155 treated with **Tre-Cz** was imaged under a confocal fluorescence microscope. Minimal fluorescence was observed prior to photoactivation (Figure 3A). After

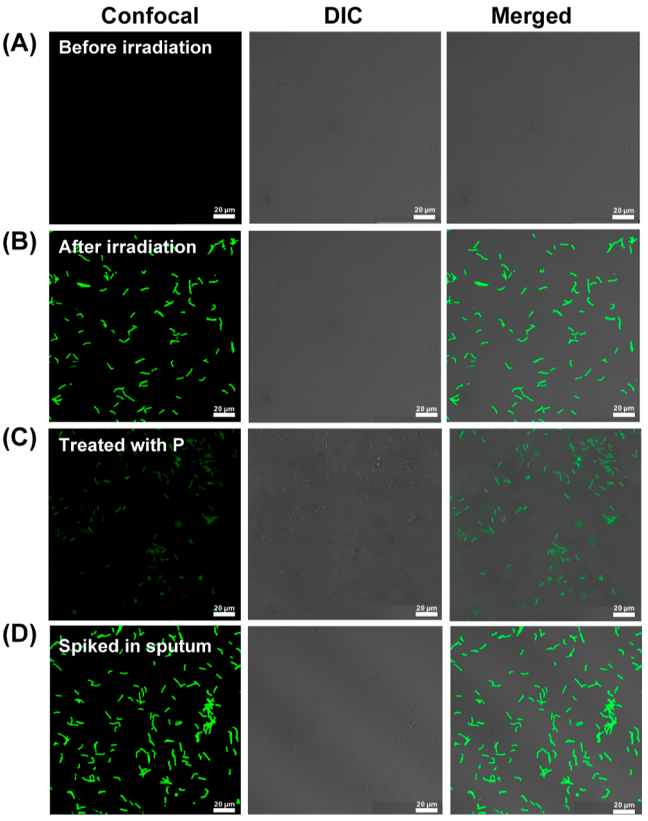

Figure 3. Fluorescence turn-on imaging of mycobacteria treated with **Tre-Cz**. Confocal fluorescence, differential interference contrast (DIC), and overlay images of *M. smegmatis* mc^{2}155 (10^8 CFU/mL) incubated with **Tre-Cz** (100 μM) (A) before and (B) after irradiation. Images were taken at the same locations in both (A,B). (C) *M. smegmatis* mc^{2}155 incubated with the photoproduct **P** (100 μM). (D) *M. smegmatis*-spiked sputum processed and incubated with **Tre-Cz** (Subject 1). Images of samples from subjects 2−5 are shown in Figure S7. Fluorescence intensities of the cell pellets and cell washes of all the five samples are shown in Figure S8. The scale bars are 20 μm.

irradiating the bacteria for 1 min, intense green fluorescence was observed, and the fluorescence was seen over the entire bacterium (Figure 3B). This implies an intracellular uptake route rather than an extracellular one, as in the latter case, the fluorescence would be seen in the mycomembrane.

When the bacteria were treated with the photoactivated product **P** at the same concentration of 100 μM, fluorescence was still observed (Figure 3C), but the intensity was 26 times lower than in the case of the fluorescence turn-on shown in Figure 3B. In the case of **Tre-Cz**, the fluorescence is masked until it is activated prior to imaging. The clear and high-contrast images demonstrate the superiority of the fluorescence turn-on probe compared to the conventional organic fluorophore.

The fast fluorescent turn-on allows the detection of mycobacteria using a handheld UV lamp for both photoactivation and visualization. To test the feasibility, *M.*

https://doi.org/10.1021/jacsau.2c00449
JACS Au 2023, 3, 1017−1028

smegmatis in the concentration range of 10^2−10^8 CFU/mL were incubated with **Tre-Cz** for 10−60 min. After washing off the excess **Tre-Cz**, the samples were irradiated for 1 min. At 30 min of incubation, the fluorescence of bacteria at concentrations of 10^3 CFU/mL and higher was clearly visible under the UV lamp (Figure S5). In the presence of *E. coli*, *S. epidermidis*, and *P. aeruginosa* (10^8 CFU/mL each), visual detection could be achieved for *M. smegmatis* at concentrations of 10^5 CFU/mL or higher (Figure S6).

2.6. Imaging Mycobacteria in Spiked Sputum

The ability of **Tre-Cz** to image mycobacteria in sputum samples was next investigated. When using sputum directly without processing, the signals were low (Figures S11−S15), likely due to the viscous matrix of unprocessed sputa, which inhibits the diffusion of **Tre-Cz** into the bacterium. The sputum was then processed using *N*-acetyl-L-cysteine/sodium hydroxide (NalC/NaOH) to digest the sputa and to reduce the growth of non-acid-fast bacilli.[69−71] The processed sputa were spiked with 10^8 CFU/mL *M. smegmatis* and then treated with **Tre-Cz**. The confocal fluorescence microscopy images were clear, showing intense green fluorescence on the bacteria and minimal background noise (Figures 3D and S7). Under the conditions of 100 μM **Tre-Cz**, 8 h of incubation and 1 min of irradiation, the lowest bacterial counts in the processed sputum that could be seen by the naked eye was 10^6 CFU/mL (Figure S9). At 10^8 CFU/mL, the fluorescence intensity continued to increase (Figure S10), whereas for bacteria in the culture medium, the fluorescence intensity plateaued at 6 h of incubation (Figure S3A). In the two control samples, *M. smegmatis*-spiked sputum without treating with **Tre-Cz** and sputum in the absence of *M. smegmatis*, the fluorescence was significantly lower (Figure S9). Taken together, these results demonstrate that both **Tre-Cz** and *M. smegmatis* are needed to observe the fluorescence.

2.7. Uptake of Tre-Cz Requires Metabolically Active Bacteria

Three experiments were carried out to test whether the uptake of **Tre-Cz** by mycobacteria requires metabolically active bacteria. Bacteria are metabolically active only when they are alive. Therefore, in the first experiment, bacteria were heated at 95 °C for 30 min, which killed the bacteria as confirmed by colony counting (Table S1). Treating the bacteria with 100 μM **Tre-Cz** did not affect the viability of the bacteria (Table S1). Compared to the untreated bacteria, the fluorescence intensity of the heat-killed bacteria decreased by 12-fold (Figure 4A).

The second experiment tested the uptake of **Tre-Cz** by log-phase vs stationary-phase bacteria. The stationary-phase bacteria were collected at the point where the bacterial growth plateaus (1.2 OD_{600}, Figure S16) and the bacterial growth slows down significantly. In this case, the fluorescence intensity was reduced to about half of that of the log-phase (0.5 OD_{600}, Figure S16) bacteria (Figure 4B).

Third, *M. smegmatis* was treated with isoniazid (INH), a TB drug that inhibits mycolic acid synthesis in mycobacteria,[72] prior to treating with **Tre-Cz**. The number of viable bacteria decreased with increasing concentrations of INH (Table S2), which in turn led to a decrease in the fluorescence intensity on the bacteria (Figure 4C).

Taken together, results in Figure 4 support that the uptake of **Tre-Cz** requires metabolically active viable mycobacteria.

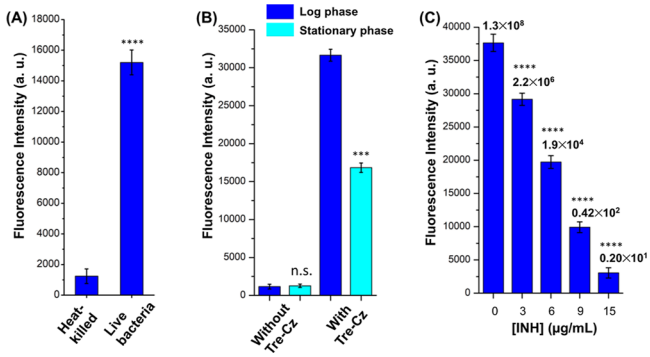

Figure 4. Uptake of **Tre-Cz** requires metabolically active bacteria: (A) heat-killed vs viable bacteria, (B) log-phase vs stationary-phase bacteria, and (C) untreated vs bacteria treated with varying concentrations of INH for 3 h. The viability of INH-treated bacteria after incubating with **Tre-Cz** was determined by plating on 7H10 agar and counting the colonies (CFU/mL). The data are shown on top of each column. In all experiments, ~10^8 CFU/mL *M. smegmatis* mc^{2}155 was used. The fluorescence intensity of bacteria only was subtracted from each data point. The data are presented as means ± SEM from three independent experiments. Data were analyzed by one-way ANOVA (*P < 0.1, **P < 0.01, ***P < 0.001, ****P < 0.0001, n.s.: not significant, and P > 0.05). Groups were compared to [INH] = 0 in (C).

2.8. Tre-Cz Hijacks Trehalose Uptake Pathways

The results clearly show the selective and specific uptake of **Tre-Cz** by mycobacteria. To test whether the uptake was through the trehalose uptake pathways, trehalose was added together with **Tre-Cz**, and the fluorescence intensity was measured at the fixed concentration of **Tre-Cz** (100 μM) and varying concentrations of trehalose. The fluorescence intensity decreased with increasing concentration of trehalose (Figure 5), indicating that **Tre-Cz** competes with trehalose for uptake.

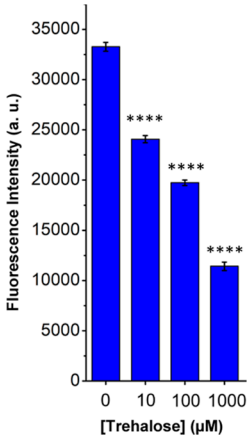

Figure 5. Fluorescence intensity of *M. smegmatis* mc^{2}155 (10^8 CFU/mL) treated with **Tre-Cz** in the presence of varying concentrations of trehalose. Data were analyzed by one-way ANOVA (****P < 0.0001). Groups were compared to [Trehalose] = 0.

When maltose was added instead of trehalose, the fluorescence intensity remained unchanged even at a high concentration of 10 mM maltose (Figure S17).

2.9. Uptake of Tre-Cz Is Independent of Ag85

The two main pathways involved in the utilization and transport of trehalose by mycobacteria are Ag85 that catalyzes

https://doi.org/10.1021/jacsau.2c00449
JACS Au 2023, 3, 1017−1028

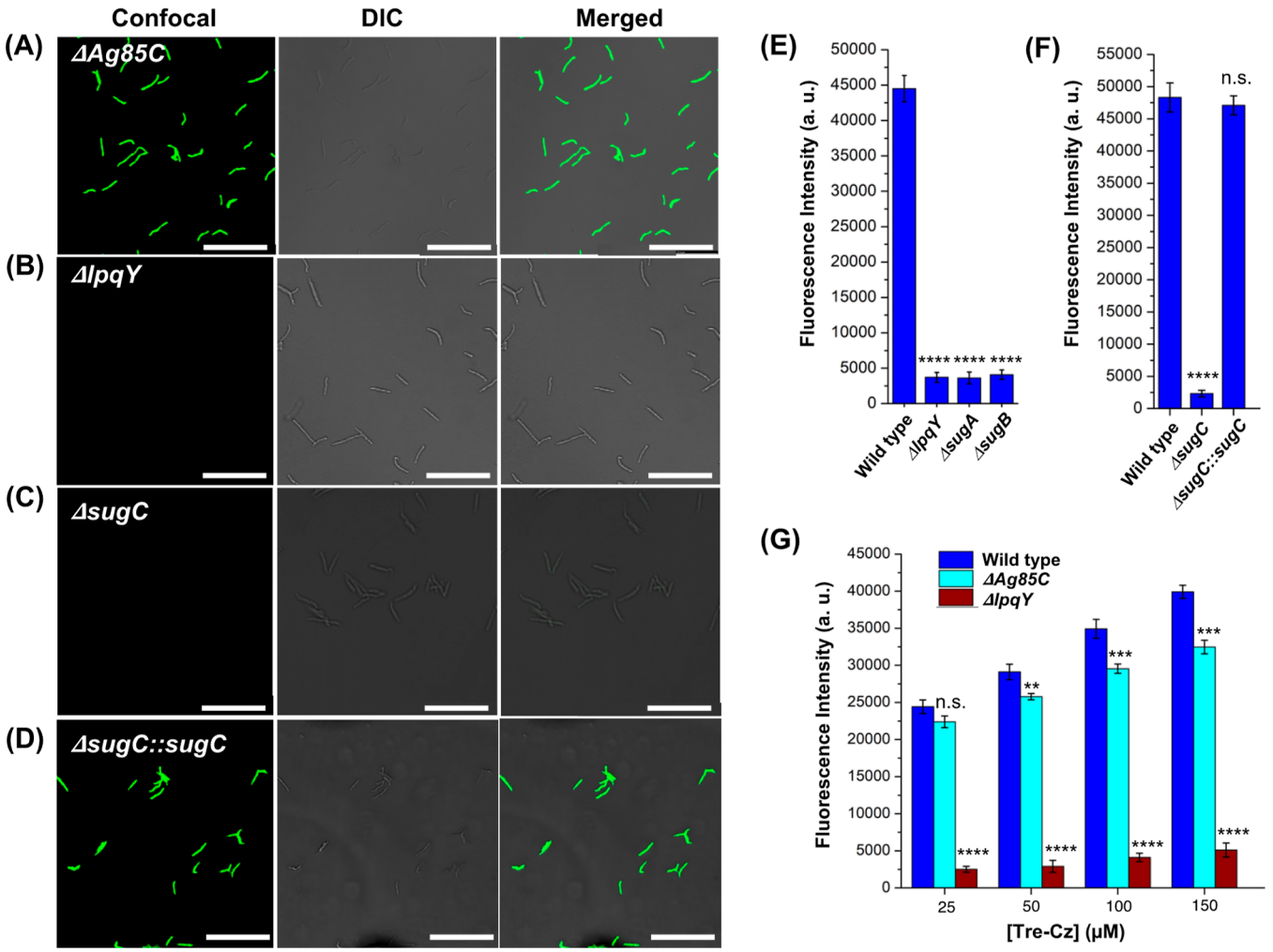

Figure 6. Confocal fluorescence microscopy images of (A) Δ*Ag85C*, (B) Δ*lpqY*, (C) Δ*sugC*, and (D) Δ*sugC::sugC* after treating with **Tre-Cz**. The scale bars are 20 μm. (E) Fluorescence intensity of *M. smegmatis* mc^{2}155 wild type, Δ*lpqY*, Δ*sugA*, and Δ*sugB* after treating with **Tre-Cz**. (F) Fluorescence intensity of *M. smegmatis* mc^{2}155 wild type, Δ*sugC*, and Δ*sugC::sugC* after treating with **Tre-Cz**. (G) Fluorescence intensity of *M. smegmatis* mc^{2}155 wild type, Δ*Ag85C*, and Δ*lpqY* after treating with different concentrations of **Tre-Cz**. In (E−G), the fluorescence intensity of the bacteria only was subtracted from each data point. The results are means ± SEM from three independent experiments. Data were analyzed by one-way ANOVA (*P < 0.1, **P < 0.01, ***P < 0.001, ****P < 0.0001, n.s.: not significant, and P > 0.05).

the transesterification of TMM to give TDM and trehalose in the periplasm and the ABC transporter LpqY-SugABC that brings trehalose from the periplasm into the cytoplasm (Scheme 1).[36,73] To test if the uptake of **Tre-Cz** is Ag85 dependent, two experiments were carried out: lipid extraction and uptake by an Ag85 deletion mutant Δ*Ag85C*.

The product of Ag85-catalyzed transesterification reaction, TDM, is incorporated into the mycomembrane.[38,74] Therefore, if **Tre-Cz** is the substrate of Ag85, one location to find the mycolate product would be the mycomembrane, and the product should be fluorescent after photoactivation. To test this, the insoluble lipids were extracted using 2:1 chloroform/methanol.[75,76] From thin-layer chromatography (TLC), none of the extracted lipid spots were fluorescent (Figure S18). No significant fluorescence was observed even at a high concentration of 5 mM **Tre-Cz**, or when the extracted lipids were further treated with 5% tetrabutylammonium hydroxide to saponify the lipids (Figure S19). One possibility is that the probe was incorporated into the glycolipids to a small degree, but it was not detectable using the extraction and analysis method tested.

We then investigated the uptake of **Tre-Cz** by an Ag85 deletion mutant Δ*Ag85C*. The Ag85 complex consists of three homologous transesterases, Ag85A, Ag85B, and Ag85C, and all can catalyze the transesterification reactions of TMM.[77] If **Tre-Cz** is the substrate of Ag85, the fluorescence should be noticeably reduced in Δ*Ag85C*. For example, Bertozzi and co-workers reported observable reduction in labeling using their solvatochromic trehalose probe in Δ*Ag85C* compared to the wild type.[44] In our case, however, strong fluorescence was still observed on Δ*Ag85C* (Figure 6A). At the concentration range of 25−150 μM, the fluorescence on Δ*Ag85C* labeled by **Tre-Cz** was reduced by 8−18% of the wild type (Table S3). Further analysis showed that the fluorescence was mostly seen in the cell pellets of Δ*Ag85C*, similar to that of the wild type (Fig. S20).

2.10. LpqY-SugABC Is the Main Pathway for the Uptake of Tre-Cz

The periplasmic trehalose is transported into the cytoplasm by the trehalose importer LpqY-SugABC. LpqY-SugABC contains five subunits (Scheme 1).[78,79] The periplasmic LpqY subunit is the primary receptor for the recognition of trehalose, which

https://doi.org/10.1021/jacsau.2c00449
JACS Au 2023, 3, 1017−1028

binds and delivers trehalose to the transporter. SugA and SugB are transmembrane proteins that translocate trehalose to the cytoplasm. The two cytoplasmic SugC subunits are responsible for ATP hydrolysis during the transport. LpqY-SugABC is highly specific for trehalose; it does not utilize monosaccharides or other disaccharides such as maltose.[36,80] Therefore, if LpqY-SugABC is involved in the transport of **Tre-Cz**, the uptake of **Tre-Cz** in the deletion mutants will be reduced compared to the wild type.

To test the hypothesis, *M. smegmatis* mc^{2}155 LpqY-SugABC deletion mutants, Δ*lpqY*, Δ*sugA*, or Δ*sugB* were treated with **Tre-Cz**, and the results were compared with the wild type. Almost no fluorescence was observed on Δ*lpqY* (Figure 6B). The fluorescence intensity was reduced by 92% on Δ*lpqY* compared to the wild type (Figure 6E and Table S4). Similar results were observed for Δ*sugA* and Δ*sugB*, where the fluorescence was reduced by 92% and 91% compared to the wild type, respectively (Figure 6E and Table S4). Further analysis showed that the fluorescence was mostly seen in the washes of Δ*lpqY*, whereas for the wild type, the fluorescence was mostly in the bacteria (Figure S21).

We further tested whether the labeling could be restored in the complemented strain of the LpqY-SugABC deletion mutant. Since LpqY-SugABC forms an operon (Scheme 1), there might possibly be polar effects on downstream genes if *lpqY*, *sugA*, or *sugB* is deleted. This means that except for the mutant in the last gene in the operon (*sugC*), which can be complemented with the *sugC* gene, bringing back just the deleted gene in the *lpqY*, *sugA*, or *sugB* mutant might not be sufficient to fully restore the wild-type phenotype. For this reason, we tested the uptake of **Tre-Cz** by the deletion mutant Δ*sugC* and its complemented strain Δ*sugC::sugC*, which fully restores the wild-type phenotype. Similar to Δ*lpqY*, almost no fluorescence was observed on Δ*sugC* (Figure 6C), and the fluorescence intensity was reduced by 95% on Δ*sugC* compared to the wild type (Figure 6E and Table S5). The fluorescence was again observed in the complemented strain Δ*sugC::sugC* (Figure 6D), and the fluorescence intensity of Δ*sugC::sugC* was 97% of the wide type (Figure 6F and Table S5). The experiments were repeated by another researcher, giving similar results, and were verified (Figure S22). Taken together, these results demonstrate that LpqY-SugABC is essential for the uptake of **Tre-Cz**.

3. DISCUSSION

The mycobacteria imaging probe **Tre-Cz** was designed based on the fluorescence turn-on property of the carbazole and the selective uptake of trehalose by mycobacteria. Both **Tre-Cz** and the negative control **Mal-Cz** can be straightforwardly synthesized from the NHS ester **IV** and amine-derivatized Tre (**V**) or Mal (**VI**) in good yields (Scheme 2). **Tre-Cz** is minimally fluorescent but became fluorescent after irradiation at 350 nm. The fluorescence turn-on is the result of the restriction of the intramolecular charge transfer in the product **P** formed through the photoinitiated C−H insertion reaction of the azide and the carbazole.[17] Since the fluorescence is turned on at the time of imaging, the probe is in the dark state during the sample processing. This reduces the light exposure during the uptake process and minimizes photobleaching that often occurs in conventional fluorescent dyes.

Tre-Cz is highly specific for mycobacteria. It does not label other Gram-positive or Gram-negative bacteria (Figure 2B) and can image mycobacteria in the presence of other bacteria. **Tre-Cz** could also label mycobacteria in sputum (Figure 3D), although the signals from unprocessed sputum were much weaker than the processed samples. The low signal is primarily due to the viscous matrix of unprocessed sputum which inhibits the diffusion of the probe into the bacteria. Nevertheless, the signals increased with increasing concentration of spiked mycobacteria, a result that is consistent with that of processed sputum samples.

The uptake of **Tre-Cz** requires metabolically active mycobacteria. The uptake was reduced in stationary-phase bacteria and was diminished when the bacteria were killed by heat or antibiotics (Figure 4). Therefore, the probe is specific for live bacteria, which eliminates the interference from dead bacteria. Compared to the solvatochromic and quencher-fluorophore trehalose probes, **Tre-Cz** has the drawback of requiring a washing step.

Trehalose competes with **Tre-Cz** for uptake in a concentration-dependent fashion (Figure 5). Further tests on the two main pathways involved in the utilization and transport of trehalose revealed that LpqY-SugABC rather than Ag85 was the dominant pathway responsible for the uptake of **Tre-Cz**. This is supported by the following results. (1) The uptake of **Tre-Cz** was significantly reduced (>90%) in the LpqY-SugABC deletion mutants, Δ*lpqY*, Δ*sugA*, Δ*sugB*, and Δ*sugC*, and the uptake was recovered in the complemented strain Δ*sugC::sugC* (Figure 6). (2) The uptake of **Tre-Cz** was only marginally reduced in the Ag85 deletion mutant Δ*Ag85C* (Figure 6). At the concentration of 100 μM, the fluorescence on Δ*Ag85C* labeled by **Tre-Cz** was reduced by 15% of the wild type (Table S3) compared to 42% in the case of Bertozzi's solvatochromic trehalose probe.[44] Furthermore, **Tre-Cz** was not detected in the lipid extracts by either fluorescence or TLC. Since Ag85 is present both in the periplasm and extracellularly near the mycomembrane,[81] **Tre-Cz** can in principle bind to Ag85 without undergoing the Ag85-catalyzed transesterification reaction. This accounts for the observed residual fluorescence on Δ*Ag85C* and also the lack of probe incorporation into the glycolipids. (3) The fluorescence on mycobacteria appears intracellular rather than in the cell envelope (Figure 3 and 6). This is in contrast to other trehalose-based imaging probes that were the substrate of Ag85. For example, Davis' fluorescein-trehalose probe,[73] Bertozzi's solvatochromic probe,[44] and Kiessling's quencher-trehalose-fluorophore probe[47] are incorporated extracellularly through the action of Ag85, which led to the observed fluorescence in the mycomembrane. In our case, the fluorescence was seen all over the mycobacterium, which is consistent with an intracellular uptake.

Only a few trehalose probes have been reported whose incorporation is known to be dependent on the trehalose transporter LpqY-SugABC. Examples include 2-, 4-, and 6-azido trehalose[40,41,43] and deoxyfluoro-D-trehalose.[42] **Tre-Cz** adds to this small library of compounds that can hijack the LpqY-SugABC transport pathway to enable intracellular incorporation of the probes.

4. CONCLUSIONS

We designed and synthesized an azide-masked and trehalose-derivatized carbazole fluorescence turn-on probe, which, upon photoactivation, was converted into a fluorescent product through a nitrene-mediated intramolecular C−H insertion reaction into the carbazole ring. The fluorescence turn-on is fast and efficient, resulting in over 90 times increase in the fluorescence intensity after irradiation with a handheld UV

https://doi.org/10.1021/jacsau.2c00449
JACS Au 2023, 3, 1017−1028

lamp for 1 min. In fact, both fluorescence turn-on and bacteria imaging can be accomplished with a handheld UV lamp within a minute or less. The probe is highly specific for mycobacteria, capable of detecting mycobacteria spiked in sputum and in the presence of other Gram-positive and Gram-negative bacteria. The uptake of **Tre-Cz** requires metabolically active bacteria; the uptake was reduced in stationary-phase and INH-treated bacteria and was completely abolished in heat-killed bacteria. The addition of trehalose reduced the uptake, implying that **Tre-Cz** hijacks the trehalose uptake pathways. Only a small reduction in the uptake of **Tre-Cz** was observed in the Δ*Ag85C* mutant, whereas the uptake was abolished in the LpqY-SugABC deletion mutants and recovered in the complemented strain. These results demonstrate that the LpqY-SugABC transporter is the primary pathway responsible for the uptake of **Tre-Cz**. The unique incorporation mechanism of **Tre-Cz** unlocks opportunities to bring molecular cargoes to mycobacteria for both fundamental studies and potential theranostic applications.

5. METHODS

5.1. General Procedure for Tre-Cz Uptake by *M. smegmatis* mc^2 155, *M. tuberculosis* H37Ra, Mutant Strains, and Δ*sugC* Complemented Strain

M. smegmatis mc^{2}155, *M. tuberculosis* H37Ra, Δ*Ag85C*, Δ*sugB*, and Δ*lpqY* were cultured in Middlebrook 7H9 until OD_{600} reached 0.5, which corresponded to ∼10^8 CFU/mL, as determined by agar plating and colony counting. Δ*sugC* was cultured in Middlebrook 7H9 supplemented with 50 mg/L hygromycin, and Δ*sugC::sugC* was cultured in Middlebrook 7H9 supplemented with 50 mg/L hygromycin and 20 mg/L apramycin. A stock solution of 1 mM **Tre-Cz** was prepared in pH 7.4 PBS buffer containing 20% DMSO. In most experiments, the following general procedure was used unless otherwise noted. To an aliquot of 900 μL of cultured bacteria in a 1.5 mL centrifuge tube, 100 μL of the **Tre-Cz** stock solution was added, which gave the **Tre-Cz** concentration of 100 μM and the final DMSO concentration of 2%. The samples were then incubated at 37 °C for 1 h while shaking at 250 rpm in the dark. After centrifugation, the supernatant containing excess **Tre-Cz** was removed, and the bacterial pellet was washed twice with PBS. The pellet was then resuspended in 200 μL of PBS and was irradiated with a 4 W handheld UV lamp at 365 nm (intensity at the sample location: 0.5 mW/cm^2) for 1 min. The samples were then transferred to a black flat-bottom 96-well plate, and the fluorescence intensities were measured using a Tecan Infinite M200PRO multimode microplate reader at an excitation of 378 nm and an emission of 545 nm. All assays were performed in triplicate, and each experiment was repeated three times.

5.2. Sample Preparation for Confocal Microscopy

To prepare samples for confocal microscopy, an equal volume of 4% paraformaldehyde in PBS was added to the bacteria and was left at room temperature for 10 min to fix the bacterial cells. The mixture was then centrifuged, and the supernatant was removed. The resulting pellet containing fixed bacterial cells was washed twice with PBS and re-dispersed in 1 mL of PBS, and 5 μL was smeared onto a precleaned microscopic glass slide. Imaging was performed on a Leica SP8 laser scanning confocal microscope with an excitation of 405 nm and an emission window of 500−600 nm. The *x*, *y*, and *z* coordinates of the confocal stage were saved, and the sample slide was irradiated with a handheld UV lamp for 1 min before being restored to its original position for imaging.

5.3. Sputum Collection, Decontamination, and Processing

Sputum specimens were freshly collected from five different test subjects, with two samples obtained from each subject. Sputum was collected early in the morning before eating or drinking, into a sterile 50 mL centrifuge tube, until 5 mL of sputum was obtained. Prior to collection, the mouth was washed with water to minimize food particle contamination of the samples. The tube was then placed in a zip bag and sealed. Decontamination of the sputum was performed according to literature protocols.[71,82] For decontamination, 2 mL of each sputum sample was mixed with an equal volume of freshly prepared decontamination solution in a 15 mL centrifuge tube. The decontamination solution was prepared by mixing 1 mL of 1% *N*-acetyl-L-cysteine in 2.9% citric acid with 1 mL of 4% NaOH. The solutions were vortexed for 10 s with the tubes inverted. Tubes were then incubated at 37 °C for 15 min before 10 mL of PBS was added to stop the decontamination process. The tubes were then centrifuged at 3000*g* for 15 min, and the supernatant was removed. The resulting pellet was washed twice with PBS and resuspended in 1 mL of PBS.

5.4. Detection of Mycobacteria in Processed Sputum

M. smegmatis mc^{2}155 (200 μL) in PBS was added to five fresh sputum samples (800 μL each) at a final concentration of 10^8 CFU/mL. The sputum was then decontaminated and processed as described above. **Tre-Cz** was added at a final concentration of 100 μM and incubated for 1 h. The samples were then centrifuged, and the supernatants were saved. The resulting pellets were washed twice with PBS and re-dispersed in PBS. Both the pellets and supernatants were irradiated with a 4 W handheld UV lamp for 1 min, and the fluorescence intensities were measured using a plate reader. Confocal images were collected on the pellets following the procedure described above.

5.5. Isolation and Analysis of Bacterial Cell Wall Lipids

A suspension of 1600 μL of *M. smegmatis* mc^{2}155 cultured to OD 0.5 was mixed with 400 μL of **Tre-Cz** to yield a final concentration of 100 μM or 5 mM. The mixture was incubated at 37 °C for 6 h before centrifugation at 3000*g* for 10 min. The resulting cell pellets were washed twice with PBS and re-suspended in 1 mL of methanol. Chloroform (2 mL) was added to the suspension, which was then vortexed and incubated at 37 °C overnight while shaking. The cell suspension was then centrifuged at 3600 rpm for 10 min, and the supernatant containing the lipids was collected to a clean sterile glass vial. The insoluble cell pellet was washed twice with 1:2 methanol/chloroform, and the resulting supernatants were combined and evaporated under vacuum. The concentrated lipid was then dissolved in 1 mL of THF. To analyze the lipid content, a 250 μL aliquot of the lipid solution was transferred to a glass vial and irradiated with a 4 W handheld UV lamp for 1 min. A volume of 30 μL was used for TLC analysis, using solvent systems of 9:1 chloroform/acetone and 9:2:1 chloroform/methanol/acetone. The TLC plates were stained with 5% sulfuric acid in ethanol before visualization. For fluorescence intensity measurement, another 200 μL of aliquot of the lipid solution was taken, and the fluorescence intensity was measured on a plate reader. Lipid saponification was carried out by adding 1 mL of 5% aqueous tetrabutylammonium hydroxide to 750 μL of each lipid solution and stirring at 100 °C for 16 h. The samples were then cooled to 24 °C and irradiated with a 4 W handheld UV lamp for 1 min.

■ ASSOCIATED CONTENT

Supporting Information

The Supporting Information is available free of charge at https://pubs.acs.org/doi/10.1021/jacsau.2c00449.

Materials and instrumentation, procedures for the synthesis of probes and reaction intermediates, characterization spectra, calculations, and additional figures and images (PDF)

■ AUTHOR INFORMATION

Corresponding Author

Mingdi Yan − *Department of Chemistry, University of Massachusetts, Lowell, Massachusetts 01854, United States;* orcid.org/0000-0003-1121-4007; Email: Mingdi_Yan@uml.edu

https://doi.org/10.1021/jacsau.2c00449
JACS Au 2023, 3, 1017−1028

Authors

Sajani H. Liyanage − *Department of Chemistry, University of Massachusetts, Lowell, Massachusetts 01854, United States*

N. G. Hasitha Raviranga − *Department of Chemistry, University of Massachusetts, Lowell, Massachusetts 01854, United States*

Julia G. Ryan − *Department of Biology and Biotechnology, Worcester Polytechnic Institute, Worcester, Massachusetts 01609, United States*

Scarlet S. Shell − *Department of Biology and Biotechnology, Worcester Polytechnic Institute, Worcester, Massachusetts 01609, United States*

Olof Ramström − *Department of Chemistry, University of Massachusetts, Lowell, Massachusetts 01854, United States; Department of Chemistry and Biomedical Sciences, Linnaeus University, SE-39182 Kalmar, Sweden;* orcid.org/0000-0002-1533-6514

Rainer Kalscheuer − *Institute of Pharmaceutical Biology and Biotechnology, Heinrich Heine University,, 40225 Duesseldorf, Germany;* orcid.org/0000-0002-3378-2067

Complete contact information is available at: https://pubs.acs.org/10.1021/jacsau.2c00449

Author Contributions

M.Y. and S.H.L. designed the experiments and wrote the manuscript. S.H.L. carried out the synthesis, characterization of all compounds, the mechanism studies, as well as the detection *in intro* and in sputum. N.G.H.R and O.R. carried out part of the confocal fluorescence imaging experiments. J.G.R. and S.S.S. sequenced and validated Δ*Ag85C*, Δ*lpqY*, Δ*sugA*, and Δ*sugB*. R.K. provided Δ*sugC* and Δ*sugC::sugC*.

Notes

The authors declare no competing financial interest.

■ ACKNOWLEDGMENTS

This project was supported in part by a grant from NIH (R15GM128164 to M.Y.). M.Y. and S.S.S. are grateful for a UMass Lowell-Worcester Polytechnic Institute Collaborative Seed Grant for the partial support of this work. We thank Harini Perera for her assistance in creating **Scheme 1**.

■ REFERENCES

(1) *Global Tuberculosis Report*; Publications of the World Health Organization, 2022.

(2) Cheon, S. A.; Cho, H. H.; Kim, J.; Lee, J.; Kim, H. J.; Park, T. J. Recent tuberculosis diagnosis toward the end TB strategy. *J. Microbiol. Methods* **2016**, *123*, 51−61.

(3) Torre-cisneros, J.; Castón, J. J.; Moreno, J.; Rivero, A.; Vidal, E.; Jurado, R.; Kindelán, J. M. Tuberculosis in the transplant candidate: importance of early diagnosis and treatment. *Transplantation* **2004**, *77*, 1376−1380.

(4) Weyer, K.; Mirzayev, F.; Migliori, G. B.; Van Gemert, W.; D'Ambrosio, L.; Zignol, M.; Floyd, K.; Centis, R.; Cirillo, D. M.; Tortoli, E.; Gilpin, C.; de Dieu Iragena, J.; Falzon, D.; Raviglione, M. Rapid molecular TB diagnosis: evidence, policy making and global implementation of Xpert MTB/RIF. *Eur. Respir. J.* **2013**, *42*, 252−271.

(5) Yang, D.; Ding, F.; Mitachi, K.; Kurosu, M.; Lee, R. E.; Kong, Y. A Fluorescent Probe for Detecting Mycobacterium tuberculosis and Identifying Genes Critical for Cell Entry. *Front. Microbiol.* **2016**, *7*, 2021.

(6) Glickman, M. S.; Jacobs, W. R., Jr. Microbial pathogenesis of Mycobacterium tuberculosis: dawn of a discipline. *Cell* **2001**, *104*, 477−485.

(7) Smith, I. Mycobacterium tuberculosis pathogenesis and molecular determinants of virulence. *Clin. Microbiol. Rev.* **2003**, *16*, 463−496.

(8) Zumla, A.; Raviglione, M.; Hafner, R.; Fordham von Reyn, C. F. Tuberculosis. *N. Engl. J. Med.* **2013**, *368*, 745−755.

(9) Nusbaum, R. J.; Calderon, V. E.; Huante, M. B.; Sutjita, P.; Vijayakumar, S.; Lancaster, K. L.; Hunter, R. L.; Actor, J. K.; Cirillo, J. D.; Aronson, J.; Gelman, B. B.; Lisinicchia, J. G.; Valbuena, G.; Endsley, J. J. Pulmonary Tuberculosis in Humanized Mice Infected with HIV-1. *Sci. Rep.* **2016**, *6*, 21522.

(10) Putt, F. A. A modified Ziehl-Neelsen method for demonstration of leprosy bacilli and other acid-fast organisms. *Am. J. Clin. Pathol.* **1951**, *21*, 92−95.

(11) Ulrichs, T.; Lefmann, M.; Reich, M.; Morawietz, L.; Roth, A.; Brinkmann, V.; Kosmiadi, G. A.; Seiler, P.; Aichele, P.; Hahn, H.; Krenn, V.; Göbel, U. B.; Kaufmann, S. H. Modified immunohistological staining allows detection of Ziehl-Neelsen-negative Mycobacterium tuberculosis organisms and their precise localization in human tissue. *J. Pathol.* **2005**, *205*, 633−640.

(12) Dheda, K.; Ruhwald, M.; Theron, G.; Peter, J.; Yam, W. C. Point-of-care diagnosis of tuberculosis: past, present and future. *Respirology* **2013**, *18*, 217−232.

(13) Zingue, D.; Weber, P.; Soltani, F.; Raoult, D.; Drancourt, M. Automatic microscopic detection of mycobacteria in sputum: a proof-of-concept. *Sci. Rep.* **2018**, *8*, 11308.

(14) Hillemann, D.; Rüsch-Gerdes, S.; Boehme, C.; Richter, E. Rapid molecular detection of extrapulmonary tuberculosis by the automated GeneXpert MTB/RIF system. *J. Clin. Microbiol.* **2011**, *49*, 1202−1205.

(15) Xie, H.; Mire, J.; Kong, Y.; Chang, M.; Hassounah, H. A.; Thornton, C. N.; Sacchettini, J. C.; Cirillo, J. D.; Rao, J. Rapid point-of-care detection of the tuberculosis pathogen using a BlaC-specific fluorogenic probe. *Nat. Chem.* **2012**, *4*, 802−809.

(16) Klymchenko, A. S. Solvatochromic and Fluorogenic Dyes as Environment-Sensitive Probes: Design and Biological Applications. *Acc. Chem. Res.* **2017**, *50*, 366−375.

(17) Xie, S.; Proietti, G.; Ramström, O.; Yan, M. Photoactivatable Fluorogens by Intramolecular C-H Insertion of Perfluoroaryl Azide. *J. Org. Chem.* **2019**, *84*, 14520−14528.

(18) Mizusawa, K.; Ishida, Y.; Takaoka, Y.; Miyagawa, M.; Tsukiji, S.; Hamachi, I. Disassembly-driven turn-on fluorescent nanoprobes for selective protein detection. *J. Am. Chem. Soc.* **2010**, *132*, 7291−7293.

(19) Kong, Y.; Yao, H.; Ren, H.; Subbian, S.; Cirillo, S. L.; Sacchettini, J. C.; Rao, J.; Cirillo, J. D. Imaging tuberculosis with endogenous beta-lactamase reporter enzyme fluorescence in live mice. *Proc. Natl. Acad. Sci. U.S.A.* **2010**, *107*, 12239−12244.

(20) Takakusa, H.; Kikuchi, K.; Urano, Y.; Sakamoto, S.; Yamaguchi, K.; Nagano, T. Design and synthesis of an enzyme-cleavable sensor molecule for phosphodiesterase activity based on fluorescence resonance energy transfer. *J. Am. Chem. Soc.* **2002**, *124*, 1653−1657.

(21) Gao, W.; Xing, B.; Tsien, R. Y.; Rao, J. Novel fluorogenic substrates for imaging beta-lactamase gene expression. *J. Am. Chem. Soc.* **2003**, *125*, 11146−11147.

(22) Kamiya, M.; Kobayashi, H.; Hama, Y.; Koyama, Y.; Bernardo, M.; Nagano, T.; Choyke, P. L.; Urano, Y. An enzymatically activated fluorescence probe for targeted tumor imaging. *J. Am. Chem. Soc.* **2007**, *129*, 3918−3929.

(23) Zlokarnik, G.; Negulescu, P. A.; Knapp, T. E.; Mere, L.; Burres, N.; Feng, L.; Whitney, M.; Roemer, K.; Tsien, R. Y. Quantitation of transcription and clonal selection of single living cells with beta-lactamase as reporter. *Science* **1998**, *279*, 84−88.

(24) Mizukami, S.; Kikuchi, K.; Higuchi, T.; Urano, Y.; Mashima, T.; Tsuruo, T.; Nagano, T. Imaging of caspase-3 activation in HeLa cells stimulated with etoposide using a novel fluorescent probe. *FEBS Lett.* **1999**, *453*, 356−360.

(25) Pham, W.; Choi, Y.; Weissleder, R.; Tung, C. H. Developing a peptide-based near-infrared molecular probe for protease sensing. *Bioconjug. Chem.* **2004**, *15*, 1403−1407.
(26) Lawrence, D. S.; Wang, Q. Seeing is believing: peptide-based fluorescent sensors of protein tyrosine kinase activity. *ChemBioChem* **2007**, *8*, 373−378.
(27) Cheng, Y.; Xie, H.; Sule, P.; Hassounah, H.; Graviss, E. A.; Kong, Y.; Cirillo, J. D.; Rao, J. Fluorogenic probes with substitutions at the 2 and 7 positions of cephalosporin are highly BlaC-specific for rapid Mycobacterium tuberculosis detection. *Angew. Chem., Int. Ed. Engl.* **2014**, *53*, 9360−9364.
(28) Kumar, G.; Narayan, R.; Kapoor, S. Chemical Tools for Illumination of Tuberculosis Biology, Virulence Mechanisms, and Diagnosis. *J. Med. Chem.* **2020**, *63*, 15308−15332.
(29) Banahene, N.; Kavunja, H. W.; Swarts, B. M. Chemical Reporters for Bacterial Glycans: Development and Applications. *Chem. Rev.* **2022**, *122*, 3336−3413.
(30) Yamagami, H.; Matsumoto, T.; Fujiwara, N.; Arakawa, T.; Kaneda, K.; Yano, I.; Kobayashi, K. Trehalose 6,6′-dimycolate (cord factor) of Mycobacterium tuberculosis induces foreign-body- and hypersensitivity-type granulomas in mice. *Infect. Immun.* **2001**, *69*, 810−815.
(31) Thanna, S.; Sucheck, S. J. Targeting the trehalose utilization pathways of Mycobacterium tuberculosis. *MedChemComm* **2016**, *7*, 69−85.
(32) Faller, M.; Niederweis, M.; Schulz, G. E. The structure of a mycobacterial outer-membrane channel. *Science* **2004**, *303*, 1189−1192.
(33) Engelhardt, H.; Heinz, C.; Niederweis, M. A tetrameric porin limits the cell wall permeability of Mycobacterium smegmatis. *J. Biol. Chem.* **2002**, *277*, 37567−37572.
(34) Hoffmann, C.; Leis, A.; Niederweis, M.; Plitzko, J. M.; Engelhardt, H. Disclosure of the mycobacterial outer membrane: cryo-electron tomography and vitreous sections reveal the lipid bilayer structure. *Proc. Natl. Acad. Sci. U.S.A.* **2008**, *105*, 3963−3967.
(35) Woodruff, P. J.; Carlson, B. L.; Siridechadilok, B.; Pratt, M. R.; Senaratne, R. H.; Mougous, J. D.; Riley, L. W.; Williams, S. J.; Bertozzi, C. R. Trehalose is required for growth of Mycobacterium smegmatis. *J. Biol. Chem.* **2004**, *279*, 28835−28843.
(36) Kalscheuer, R.; Weinrick, B.; Veeraraghavan, U.; Besra, G. S.; Jacobs, W. R., Jr. Trehalose-recycling ABC transporter LpqY-SugA-SugB-SugC is essential for virulence of Mycobacterium tuberculosis. *Proc. Natl. Acad. Sci. U.S.A.* **2010**, *107*, 21761−21766.
(37) Furze, C. M.; Delso, I.; Casal, E.; Guy, C. S.; Seddon, C.; Brown, C. M.; Parker, H. L.; Radhakrishnan, A.; Pacheco-Gomez, R.; Stansfeld, P. J.; Angulo, J.; Cameron, A. D.; Fullam, E. Structural basis of trehalose recognition by the mycobacterial LpqY-SugABC transporter. *J. Biol. Chem.* **2021**, *296*, 100307.
(38) Backus, K. M.; Boshoff, H. I.; Barry, C. S.; Boutureira, O.; Patel, M. K.; D'Hooge, F.; Lee, S. S.; Via, L. E.; Tahlan, K.; Barry, C. E.; Davis, B. G. Uptake of unnatural trehalose analogs as a reporter for Mycobacterium tuberculosis. *Nat. Chem. Biol.* **2011**, *7*, 228−235.
(39) Kalera, K.; Stothard, A. I.; Woodruff, P. J.; Swarts, B. M. The role of chemoenzymatic synthesis in advancing trehalose analogues as tools for combatting bacterial pathogens. *Chem. Commun.* **2020**, *56*, 11528−11547.
(40) Swarts, B. M.; Holsclaw, C. M.; Jewett, J. C.; Alber, M.; Fox, D. M.; Siegrist, M. S.; Leary, J. A.; Kalscheuer, R.; Bertozzi, C. R. Probing the mycobacterial trehalome with bioorthogonal chemistry. *J. Am. Chem. Soc.* **2012**, *134*, 16123−16126.
(41) Pohane, A. A.; Moore, D. J.; Lepori, I.; Gordon, R. A.; Nathan, T. O.; Gepford, D. M.; Kavunja, H. W.; Swarts, B. M.; Siegrist, M. S. A Bifunctional Chemical Reporter for in Situ Analysis of Cell Envelope Glycan Recycling in Mycobacteria. *ACS Infect. Dis.* **2022**, *8*, 2223−2231.
(42) Rundell, S. R.; Wagar, Z. L.; Meints, L. M.; Olson, C. D.; O'Neill, M. K.; Piligian, B. F.; Poston, A. W.; Hood, R. J.; Woodruff, P. J.; Swarts, B. M. Deoxyfluoro-d-trehalose (FDTre) analogues as potential PET probes for imaging mycobacterial infection. *Org. Biomol. Chem.* **2016**, *14*, 8598−8609.
(43) Parker, H. L.; Tomás, R. M. F.; Furze, C. M.; Guy, C. S.; Fullam, E. Asymmetric trehalose analogues to probe disaccharide processing pathways in mycobacteria. *Org. Biomol. Chem.* **2020**, *18*, 3607−3612.
(44) Kamariza, M.; Shieh, P.; Ealand, C. S.; Peters, J. S.; Chu, B.; Rodriguez-Rivera, F. P.; Babu Sait, M. R.; Treuren, W. V.; Martinson, N.; Kalscheuer, R.; Kana, B. D.; Bertozzi, C. R. Rapid detection of Mycobacterium tuberculosis in sputum with a solvatochromic trehalose probe. *Sci. Transl. Med.* **2018**, *10*, No. eaam6310.
(45) Sahile, H. A.; Rens, C.; Shapira, T.; Andersen, R. J.; Av-Gay, Y. DMN-Tre Labeling for Detection and High-Content Screening of Compounds against Intracellular Mycobacteria. *ACS Omega* **2020**, *5*, 3661−3669.
(46) Kamariza, M.; Keyser, S. G. L.; Utz, A.; Knapp, B. D.; Ealand, C.; Ahn, G.; Cambier, C. J.; Chen, T.; Kana, B.; Huang, K. C.; Bertozzi, C. R. Toward Point-of-Care Detection of Mycobacterium tuberculosis: A Brighter Solvatochromic Probe Detects Mycobacteria within Minutes. *JACS Au* **2021**, *1*, 1368−1379.
(47) Hodges, H. L.; Brown, R. A.; Crooks, J. A.; Weibel, D. B.; Kiessling, L. L. Imaging mycobacterial growth and division with a fluorogenic probe. *Proc. Natl. Acad. Sci. U.S.A.* **2018**, *115*, 5271−5276.
(48) Banahene, N.; Gepford, D. M.; Biegas, K. J.; Swanson, D. H.; Hsu, Y. P.; Murphy, B. A.; Taylor, Z. E.; Lepori, I.; Siegrist, M. S.; Obregón-Henao, A.; Van Nieuwenhze, M. S.; Swarts, B. M. A Far-Red Molecular Rotor Fluorogenic Trehalose Probe for Live Mycobacteria Detection and Drug-Susceptibility Testing. *Angew. Chem., Int. Ed. Engl.* **2023**, *62*, No. e202213563.
(49) Holmes, N. J.; Kavunja, H. W.; Yang, Y.; Vannest, B. D.; Ramsey, C. N.; Gepford, D. M.; Banahene, N.; Poston, A. W.; Piligian, B. F.; Ronning, D. R.; Ojha, A. K.; Swarts, B. M. A FRET-Based Fluorogenic Trehalose Dimycolate Analogue for Probing Mycomembrane-Remodeling Enzymes of Mycobacteria. *ACS Omega* **2019**, *4*, 4348−4359.
(50) Li, X.; Geng, P.; Hong, X.; Sun, Z.; Liu, G. Detecting Mycobacterium Tuberculosis using a nitrofuranyl calanolide-trehalose probe based on nitroreductase Rv2466c. *Chem. Commun.* **2021**, *57*, 13174−13177.
(51) Liu, L. H.; Yan, M. Perfluorophenyl azides: new applications in surface functionalization and nanomaterial synthesis. *Acc. Chem. Res.* **2010**, *43*, 1434−1443.
(52) Xie, S.; Sundhoro, M.; Houk, K. N.; Yan, M. Electrophilic Azides for Materials Synthesis and Chemical Biology. *Acc. Chem. Res.* **2020**, *53*, 937−948.
(53) Chen, X.; Wu, B.; Jayawardana, K. W.; Hao, N.; Jayawardena, H. S.; Langer, R.; Jaklenec, A.; Yan, M. Magnetic Multivalent Trehalose Glycopolymer Nanoparticles for the Detection of Mycobacteria. *Adv. Healthcare Mater.* **2016**, *5*, 2007−2012.
(54) Wijesundera, S. A.; Jayawardana, K. W.; Yan, M. Trehalose-Modified Silver Nanoparticles as Antibacterial Agents with Reduced Cytotoxicity and Enhanced Uptake by Mycobacteria. *ACS Appl. Nano Mater.* **2022**, *5*, 10704−10714.
(55) Wijesundera, S. A.; Liyanage, S. H.; Biswas, P.; Reuther, J. F.; Yan, M. Trehalose-Grafted Glycopolymer: Synthesis via the Staudinger Reaction and Capture of Mycobacteria. *Biomacromolecules* **2023**, *24*, 238−245.
(56) Al-Bataineh, S. A.; Luginbuehl, R.; Textor, M.; Yan, M. Covalent immobilization of antibacterial furanones via photochemical activation of perfluorophenylazide. *Langmuir* **2009**, *25*, 7432−7437.
(57) Wu, B.; Ndugire, W.; Chen, X.; Yan, M. Maltoheptaose-Presenting Nanoscale Glycoliposomes for the Delivery of Rifampicin to E. coli. *ACS Appl. Nano Mater.* **2021**, *4*, 7343−7357.
(58) Ndugire, W.; Truong, D.; Hasitha Raviranga, N. G.; Lao, J.; Ramström, O.; Yan, M. Turning on the Antimicrobial Activity of Gold Nanoclusters Against Multidrug-Resistant Bacteria. *Angew. Chem., Int. Ed. Engl.* **2023**, *2023*, No. e202214086.

https://doi.org/10.1021/jacsau.2c00449
JACS Au 2023, 3, 1017−1028

(59) Wu, B.; Yang, X.; Yan, M. Synthesis and Structure-Activity Relationship Study of Antimicrobial Auranofin against ESKAPE Pathogens. *J. Med. Chem.* **2019**, *62*, 7751−7768.
(60) Lee, H. L.; Lord, S. J.; Iwanaga, S.; Zhan, K.; Xie, H.; Williams, J. C.; Wang, H.; Bowman, G. R.; Goley, E. D.; Shapiro, L.; Twieg, R. J.; Rao, J.; Moerner, W. E. Superresolution imaging of targeted proteins in fixed and living cells using photoactivatable organic fluorophores. *J. Am. Chem. Soc.* **2010**, *132*, 15099−15101.
(61) Lord, S. J.; Conley, N. R.; Lee, H. L.; Samuel, R.; Liu, N.; Twieg, R. J.; Moerner, W. E. A photoactivatable push-pull fluorophore for single-molecule imaging in live cells. *J. Am. Chem. Soc.* **2008**, *130*, 9204−9205.
(62) Sparks, I. L.; Derbyshire, K. M.; Jacobs, W. R., Jr.; Morita, Y. S. Mycobacterium smegmatis: The Vanguard of Mycobacterial Research. *J. Bacteriol.* **2023**, *205*, No. e0033722.
(63) Bansal-Mutalik, R.; Nikaido, H. Mycobacterial outer membrane is a lipid bilayer and the inner membrane is unusually rich in diacyl phosphatidylinositol dimannosides. *Proc. Natl. Acad. Sci. U.S.A.* **2014**, *111*, 4958−4963.
(64) Brennan, P. J.; Nikaido, H. The envelope of mycobacteria. *Annu. Rev. Biochem.* **1995**, *64*, 29−63.
(65) Marrakchi, H.; Lanéelle, M. A.; Daffé, M. Mycolic acids: structures, biosynthesis, and beyond. *Chem. Biol.* **2014**, *21*, 67−85.
(66) Zuber, B.; Chami, M.; Houssin, C.; Dubochet, J.; Griffiths, G.; Daffé, M. Direct visualization of the outer membrane of mycobacteria and corynebacteria in their native state. *J. Bacteriol.* **2008**, *190*, 5672−5680.
(67) De Smet, K. A. L.; Weston, A.; Brown, I. N.; Young, D. B.; Robertson, B. D. Three pathways for trehalose biosynthesis in mycobacteria. *Microbiology* **2000**, *146*, 199−208.
(68) Heinrichs, M. T.; May, R. J.; Heider, F.; Reimers, T.; Sy, B. S.; Peloquin, C. A.; Derendorf, H. Mycobacterium tuberculosis Strains H37ra and H37rv have equivalent minimum inhibitory concentrations to most antituberculosis drugs. *Int. J. Mycobact.* **2018**, *7*, 156−161.
(69) De Bel, A.; De Geyter, D.; De Schutter, I.; Mouton, C.; Wellemans, I.; Hanssens, L.; Schelstraete, P.; Malfroot, A.; Pierard, D. Sampling and decontamination method for culture of nontuberculous mycobacteria in respiratory samples of cystic fibrosis patients. *J. Clin. Microbiol.* **2013**, *51*, 4204−4206.
(70) Stephenson, D.; Perry, A.; Nelson, A.; Robb, A. E.; Thomas, M. F.; Bourke, S. J.; Perry, J. D.; Jones, A. L. Decontamination Strategies Used for AFB Culture Significantly Reduce the Viability of Mycobacterium abscessus Complex in Sputum Samples from Patients with Cystic Fibrosis. *Microorganisms* **2021**, *9*, 1597.
(71) Kubica, G. P.; Dye, W. E.; Cohn, M. L.; Middlebrook, G. Sputum digestion and decontamination with N-acetyl-L-cysteine-sodium hydroxide for culture of mycobacteria. *Am. Rev. Respir. Dis.* **1963**, *87*, 775−777.
(72) Timmins, G. S.; Deretic, V. Mechanisms of action of isoniazid. *Mol. Microbiol.* **2006**, *62*, 1220−1227.
(73) Backus, K. M.; Boshoff, H. I.; Barry, C. S.; Boutureira, O.; Patel, M. K.; D'Hooge, F.; Lee, S. S.; Via, L. E.; Tahlan, K.; Barry, C. E., 3rd; Davis, B. G. Uptake of unnatural trehalose analogs as a reporter for Mycobacterium tuberculosis. *Nat. Chem. Biol.* **2011**, *7*, 228−235.
(74) Farr, T. D.; Lai, C. H.; Grünstein, D.; Orts-Gil, G.; Wang, C. C.; Boehm-Sturm, P.; Seeberger, P. H.; Harms, C. Imaging early endothelial inflammation following stroke by core shell silica superparamagnetic glyconanoparticles that target selectin. *Nano Lett.* **2014**, *14*, 2130−2134.
(75) Foley, H. N.; Stewart, J. A.; Kavunja, H. W.; Rundell, S. R.; Swarts, B. M. Bioorthogonal Chemical Reporters for Selective In Situ Probing of Mycomembrane Components in Mycobacteria. *Angew. Chem., Int. Ed. Engl.* **2016**, *55*, 2053−2057.
(76) Dutta, A. K.; Choudhary, E.; Wang, X.; Záhorszka, M.; Forbak, M.; Lohner, P.; Jessen, H. J.; Agarwal, N.; Korduláková, J.; Jessen-Trefzer, C. Trehalose Conjugation Enhances Toxicity of Photosensitizers against Mycobacteria. *ACS Cent. Sci.* **2019**, *5*, 644−650.
(77) Belisle, J. T.; Vissa, V. D.; Sievert, T.; Takayama, K.; Brennan, P. J.; Besra, G. S. Role of the major antigen of Mycobacterium tuberculosis in cell wall biogenesis. *Science* **1997**, *276*, 1420−1422.
(78) Cole, S. T.; Brosch, R.; Parkhill, J.; Garnier, T.; Churcher, C.; Harris, D.; Gordon, S. V.; Eiglmeier, K.; Gas, S.; Barry, C. E., 3rd; Tekaia, F.; Badcock, K.; Basham, D.; Brown, D.; Chillingworth, T.; Connor, R.; Davies, R.; Devlin, K.; Feltwell, T.; Gentles, S.; Hamlin, N.; Holroyd, S.; Hornsby, T.; Jagels, K.; Krogh, A.; McLean, J.; Moule, S.; Murphy, L.; Oliver, K.; Osborne, J.; Quail, M. A.; Rajandream, M. A.; Rogers, J.; Rutter, S.; Seeger, K.; Skelton, J.; Squares, R.; Squares, S.; Sulston, J. E.; Taylor, K.; Whitehead, S.; Barrell, B. G. Deciphering the biology of Mycobacterium tuberculosis from the complete genome sequence. *Nature* **1998**, *393*, 537−544.
(79) Liu, F.; Liang, J.; Zhang, B.; Gao, Y.; Yang, X.; Hu, T.; Yang, H.; Xu, W.; Guddat, L. W.; Rao, Z. Structural basis of trehalose recycling by the ABC transporter LpqY-SugABC. *Sci. Adv.* **2020**, *6*, No. eabb9833.
(80) Wolber, J. M.; Urbanek, B. L.; Meints, L. M.; Piligian, B. F.; Lopez-Casillas, I. C.; Zochowski, K. M.; Woodruff, P. J.; Swarts, B. M. The trehalose-specific transporter LpqY-SugABC is required for antimicrobial and anti-biofilm activity of trehalose analogues in Mycobacterium smegmatis. *Carbohydr. Res.* **2017**, *450*, 60−66.
(81) Jackson, M.; Stevens, C. M.; Zhang, L.; Zgurskaya, H. I.; Niederweis, M. Transporters Involved in the Biogenesis and Functionalization of the Mycobacterial Cell Envelope. *Chem. Rev.* **2021**, *121*, 5124−5157.
(82) Morcillo, N.; Imperiale, B.; Palomino, J. C. New simple decontamination method improves microscopic detection and culture of mycobacteria in clinical practice. *Infect. Drug Resist.* **2008**, *1*, 21−26.

https://doi.org/10.1021/jacsau.2c00449
JACS Au 2023, 3, 1017−1028